Senior Fresh Computational Physics Laboratory Report

The Zeeman effect

Author: Aaron Miller
173222856
Partner: Patrick Sinnot

February 10, 2020

In this experiment, we investigate the electron transition of the Cadmium atom from $5^1D_2 \rightarrow 5^1P_1$. We found the wavelenght of the Cadmium red line we were investigating to be $\lambda = (657.67 \pm 15.98)nm$ in good agreement with the actual value of $\lambda = 643.8nm$[1]. We then applied a magnetic field, and observed a splitting of the spectral lines. This was the normal Zeeman effect. Initially we investigated the transverse Zeeman effect, where the magnetic field is perpendicular to the axis the light propagates along. . We found the product of the radius of our peaks by the shift between them to be effectively constant for a given current $\iff$ magnetic field. The Bohr magneton was determined to be $\mu_B = (9.4845 \pm 1.3032) \times 10^{-24} JT^{-1}$, which is within the expected value of $\mu_B = 9.274 \times 10^{-24} JT^{-1}$. Values for the shift in wavelenght were found to be $\Delta\lambda = (9.145 \pm 0.283)pm, (11.22 \pm 0.355)pm$ for I=5,7A. The light from the outer most peaks were perpendicularily to the inner peak. For the Longitudinal Zeeman effect, we moved the magnet so the magnetic field is parallel to the axis the light propagates along.

Contents

1 Introduction

1.1 Atomic States

From quantum mechanics we know that the total angular momentum $\mathbf{J}$, total orbital $\mathbf{L}$ and total spin $\mathbf{S}$ momenta are related by

$$\mathbf{J} = \mathbf{L} + \mathbf{S}. \tag{1.1}$$

The eigenvalues of these operators are

$$\mathbf{S}^2 \to \hbar^2 S(S+1), \quad S \in Z/2, \tag{1.2}$$

$$\mathbf{L}^2 \to \hbar^2 L(L+1), \quad L \in Z, \tag{1.3}$$

$$\mathbf{J}^2 \to \hbar^2 J(J+1), \quad |S-L| \leq J \leq |S+L|. \tag{1.4}$$

In an atom, the Hamiltonian of the system in a magnetic field is given by

$$H = H_0 + V_M, \tag{1.5}$$

where V_M is the perturbation to the Hamiltonian H_0 of the electric field, given by the inner product of the magnetic moment and the magnetic field

$$V_M = \vec{\mu} \cdot \vec{B}, \quad \vec{\mu} = -\frac{\mu_{\mathrm{B}} g \vec{J}}{\hbar}, \quad g = 1 + \frac{J(J+1) + S(S+1) - L(L+1)}{2J(J+1)} \tag{1.6}$$

with μ_B being the Bohr magneton, and g is the Landé g-factor. We have

We often consider only the z-component of the total angular momentum $\mathbf{J}_z$, M_J. It is clear that there are (2J+1) M_J eigenvalues,

$$M_J \in -J, ..., 0, ...J \tag{1.7}$$

Now if we consider a magnetic field in the z-direction, 1.6 simplifies to

$$V_M = -M_J g \mu_B \tag{1.8}$$

1.2 Spectra

Due to the emission of energy in the form of photons in the transition between angular momentum states, we observe distinct spectral lines. Theses lines are due to the interaction of the dipole moment $\vec{P}$ and the electric field $\vec{E}$, given by

$$E_{int} = -\vec{P} \cdot \vec{E}. \tag{1.9}$$

These interactions are aptly named as 'Electric dipole transitions'. The relevant transition rules which govern the spin-1 photons emitted are:

- $\Delta J = \pm 1, 0$, $\Delta M_J = \pm 1, 0$ due to conservation of angular momentum with the photon [transition between two J=0 systems is not allowed]
- Spin state, $\Delta S = 0$

1.3 The Zeeman Effect

The Zeeman effect is a purely quantum mechanical effect which is caused due to the interaction between the static magnetic field $\vec{B}$, and the angular momentum of an atom. The change in energy V_M to the unperturbed Hamiltonian H_0 causes a splitting of spectral lines from certain atoms. In considering the z-component as in 1.8, we see that the field quantizes the energy into (2J+1) levels corrosponding to the allowed M_J values. When there is no field, all these states are degenerate: the (2J+1) states have the same energy. Lifting this degeneracy is the Zeeman effect, and it results in the spectral lines described in section 1.2. Note that that the Zeeman effect occurs for when the interaction term V_M is very small. If the magnetic field is large enough, it disrupts the orbital and spin angular momentum coupling, which results in a different pattern of spectral splitting then the normal Zeeman effect. This is the Paschen-Bach effect [3].

Now there are two cases of the Zeeman effect

- Normal Zeeman effect which occurs when S=0 [ironically the less commonly observed effect].
- Anomalous Zeeman effect which occurs when S≠0

We shall for this experiment be considering the normal Zeeman effect. This evident in the state transitions $5^1D_2(S = 0, L = 2, J = 2) \rightarrow 5^1P_1(S = 0, L = 1, J = 1)$ in Cadmium. For the purposes of this experiment, we will investigate this Cadmium transition.'When we apply a magnetic field, this transition releases energy ΔE according to M_J in Eq.1.8. The allowed values of the change in M_J are illustrated in figure 1.1 below.

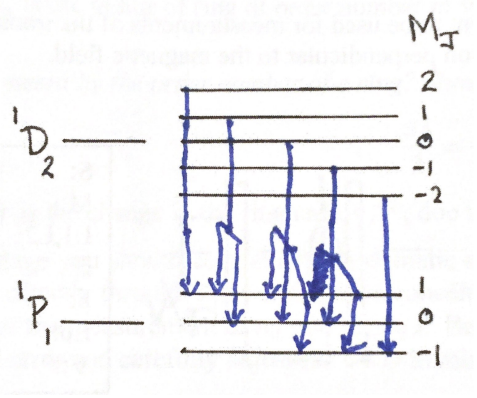

Figure 1.1: Allowed values of ΔM_J in the transition $5^1D_2 \rightarrow 5^1P_1$

Each branch in this figure corresponds to a different value of ΔE, with a change in wavelenght to the observed spectra of

$$\Delta\lambda = \frac{\lambda_0^2 \mu_B B}{hc}. \tag{1.10}$$

1.4 Polarisation of spectra

- For $\Delta M = 0$, this is classically equivalent to a dipole oscillating parallel to the magnetic field [in the z-direction]. No photons are emitted in the z-direction, and the light emitted is linearly polarized when viewed from the x-y plane.[Transverse Zeeman Effect]
- For $\Delta M = \pm 1$, the emitted spectra travel in the direction of the magnetic field. This corresponds to two parallel dipoles oscillating with a 90° phase difference between them. The light is circularly polarised. [Longitudinal Zeeman Effect]

1.5 Note of spectroscopic notation

This method of notation is in the form of $N^{2S+1}L_J$, where L, S, and J are the orbital, spin, and total angular momenta. N is the principal quantum number [often omitted]. For L=0,1,2,3.. we use S,P,D,F... .

2 Methodology

2.1 Experimental setup theory

The figure below shows the experimental setup used

Figure 2.1: Experimental setup

A filter is used so only red light can be visible [and so blue light which is also emmited can not be seen]. The Fabry Perot Etalon is made of many parallel alminuized glass plates so that as light passes through it, it is reflected back and forth several times with partial emission each time when the light is in resonance with it. On the other side of the Etalon, the light interferes constructively. The path difference is given by

$$\Delta = 2nd\cos\beta,$$

where $\Delta = m\lambda$ for m an integer, and being the condition for constructive interference and visible fringes. Also, we find that the radius of the mth ring is given by

$$m\lambda = 2nd\left(1 - \frac{r_m^2}{2n^2f^2}\right),$$

and upon differentiating,

$$\frac{\Delta\lambda}{\lambda} = -\frac{r\Delta r}{n^2f^2}. \tag{2.1}$$

Proofs for the previous assertions are included in the appendix.
In order to determine the polarity of the light, we used a linear, and $\lambda/4$ polariser.

- To determine if the light is liberally polarised, we turned the polarising plane to 90° . If the intensity dropped to 0, it is liberally polarised.
- The $\lambda/4$ wave plate has the effect of shifting the component of the electric field parallel to the direction of propagation by 90° with respect to the perpendicular component.

3 Method

Note, most measurements were in pixels so we used the formula

$$\Delta x = \Delta p \times 14um \tag{3.1}$$

to convert measurements.

3.1 To determine the wavelength of the red line in Cadmium

Initially we viewed the ring pattern through the eyepiece [FIG.2.1], and then calibrated the CCD camera to make sure we were getting sensible results. To do this we set the camera resolution to 256 pixels, as we did not have enough computation power to get real time results with higher resolutions. When the spectrum was ledgible, we switched to 2048 to get a clear view of the peaks [See Appendix section for graphs].

On rearranging Eq.2.1 to get

$$r_m^2 = 2n^2f^2 - \frac{\lambda f^2 n}{d} \cdot m. \tag{3.2}$$

From the slope of a graph of the order of images, against r^2 we can obtain a value of the wavelength as we are given all other constants. We achieved this by measuring the distance from the center of the peaks, to the center of the mth order peak. We converted our measurements from pixels to meters using Eq.3.1. An average of the RHS, and LHS orders was taken to reduce error.

3.2 Transverse Zeeman Effect

For this section, we apply a static magnetic field to the apparatus, using a high current power supply. We set the voltage to a max, and the current to a minimum to begin with. We set the supply to 'constant current mode' to combat the heat acquired from increased resistance. We began by observing triplet lines through the eyepiece to assure ourselves that the apparatus was configured.

We measured r, the distance to the center of the distribution and Δr, the distance between the left and right peaks of the central peak. We did this for different values of the current.

Combining previous equations, we find

$$r\Delta r = \frac{n^2 f^2 B \lambda \mu_B}{hc}. \tag{3.3}$$

Now the slope of a plot of $r\Delta r$ against B will reveal μ_B.

Using the polariser, I noted the effect of different angles.

3.3 Longitudinal Zeeman Effect

I rotated the cadmium, and magnetic coils $90^{c}irc$ in so the field was pointing directly at the eyepiece. We then repeated the methodology of the previous section, however we used a combination of first the polariser, and then the 1/4 wave plate to investigate the polarisation state.

4 Results

The constants we were given are summerised here

	Value
d	4.0×10^{-3}m
n	1.457
f^2	2.25×10^{-2}m^2

4.1 To determine the wavelength of the red line in Cadmium

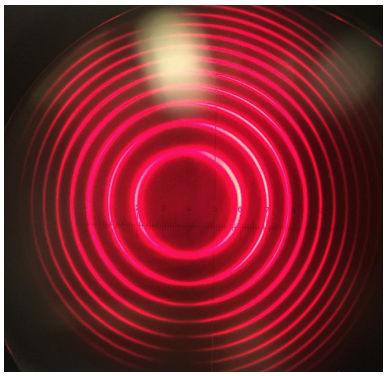

Figure 4.1: Spectral lines for B=0

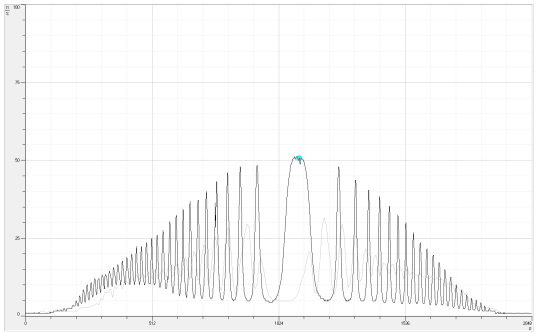

Figure 4.2: Spectral lines intensitys for B=0

Figure 4.1, and 6.1 illustrates the expected spectral lines from the caesium transition. The radii of the first nine rings to the left and right were taken. The data is below.

Calculation of R^2 for $\|\vec{B}\| = 0$			
ΔP(pixels)	ΔX(m)	R^2(m)	δR^2(m)^2
165	2.31×10^{-3}	5.3361×10^{-6}	9.84×10^{-8}
233	3.262×10^{-3}	$1.064\,06 \times 10^{-5}$	1.346×10^{-7}
288	4.032×10^{-3}	1.6257×10^{-5}	1.63×10^{-7}
332	4.648×10^{-3}	$2.160\,39 \times 10^{-5}$	1.871×10^{-7}
371	5.194×10^{-3}	2.697×10^{-5}	2.084×10^{-7}
406	5.684×10^{-3}	3.23×10^{-5}	2.273×10^{-7}
439	6.146×10^{-3}	3.777×10^{-5}	2.448×10^{-7}
469	6.566×10^{-3}	4.3112×10^{-5}	2.614×10^{-7}
497	6.958×10^{-3}	4.841×10^{-5}	2.758×10^{-7}

Now, on plotting this data we find the slope to be

$$k = (5.3913 \pm 0.0090) \times 10^{-6} \quad \iff \lambda = \frac{d}{nf^2}k = (6.5767 \pm 0.1598)m$$

The figure below shows the plot.

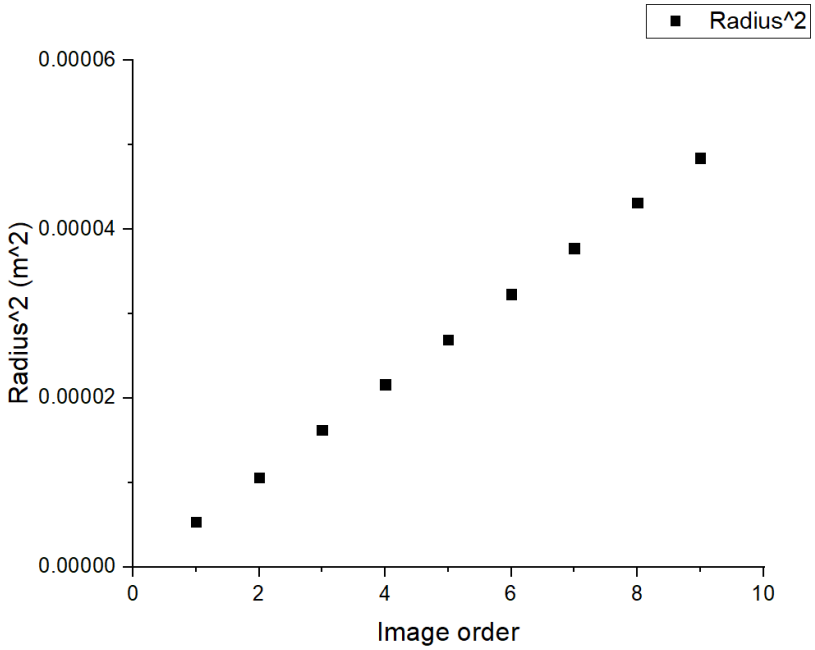

Figure 4.3: Graph of r^2 against image order

4.2 Transverse Zeeman Effect

In this section we observed the splitting into triple peaks, see the appendix for intensity plots. We are given the magnetic field strength, as a function of increasing current

[which is measurable from the power supply]. This differs from the decreasing current due to a hysteresis loop ie: lingering magnetisation.

I	B(T)
4	0.394
5	0.485
6	0.552
7	0.594

(4.1)

Now, data was taken as described previously for each value of current I. I include tables for each of these values of I below.

Calculation of $R\Delta R$ for I = 4A			
ΔP(pixels)	R(m)	(m)	$R\Delta R$
133	1.862×10^{-3}	2.8×10^{-4}	5.2136×10^{-7}
211	2.954×10^{-3}	1.68×10^{-4}	4.962×10^{-7}
267	3.738×10^{-3}	1.33×10^{-4}	4.971×10^{-7}
313	4.382×10^{-3}	1.12×10^{-4}	4.907×10^{-7}
136	1.904×10^{-3}	2.87×10^{-4}	5.464×10^{-7}
214	2.996×10^{-3}	1.75×10^{-4}	5.243×10^{-7}
270	3.78×10^{-3}	9.8×10^{-5}	3.704×10^{-7}
316	4.424×10^{-3}	1.05×10^{-4}	4.6452×10^{-7}

Figure 4.4: I=4A

Calculation of $R\Delta R$ for I = 5A			
ΔP(pixels)	R(m)	(m)	$R\Delta R$
142	1.988×10^{-3}	3.57×10^{-4}	7.097×10^{-7}
222	3.105×10^{-3}	2.17×10^{-4}	6.740×10^{-7}
265	3.71×10^{-3}	1.61×10^{-4}	5.970×10^{-7}
324	4.538×10^{-3}	1.47×10^{-4}	6.686×10^{-7}
122	1.308×10^{-3}	3.64×10^{-4}	6.210×10^{-7}
216	3.024×10^{-3}	2.12×10^{-4}	6.411×10^{-7}
258	3.612×10^{-3}	1.75×10^{-4}	6.321×10^{-7}
315	4.41×10^{-3}	7×10^{-5}	7.235×10^{-7}

Figure 4.5: I=5A

Calculation of $R\Delta R$ for I = 6A			
ΔP(pixels)	R(m)	(m)	$R\Delta R$
143	2.002×10^{-3}	4.2×10^{-4}	8.402×10^{-7}
222	3.108×10^{-3}	2.52×10^{-4}	7.832×10^{-7}
278	3.892×10^{-3}	1.96×10^{-4}	7.628×10^{-7}
324	4.536×10^{-3}	1.68×10^{-4}	7.621×10^{-7}
127	1.778×10^{-3}	4.06×10^{-4}	7.218×10^{-7}
205	2.87×10^{-3}	2.52×10^{-4}	7.231×10^{-7}
261	3.654×10^{-3}	1.96×10^{-4}	6.321×10^{-7}
308	4.312×10^{-3}	1.68×10^{-4}	7.235×10^{-7}

Figure 4.6: I=6A

Calculation of $R\Delta R$ for I = 7A			
ΔP(pixels)	R(m)	(m)	$R\Delta R$
121	1.694×10^{-3}	5.39×10^{-4}	9.1306×10^{-7}
206	2.884×10^{-3}	2.8×10^{-4}	6.258×10^{-7}
264	3.696×10^{-3}	2.17×10^{-4}	8.02×10^{-7}
311	4.354×10^{-3}	4.354×10^{-4}	7.92×10^{-7}
118	1.652×10^{-3}	1.652×10^{-4}	8.44×10^{-7}
202	2.828×10^{-3}	2.828×10^{-4}	8.44×10^{-7}
260	3.64×10^{-3}	3.64×10^{-4}	7.91×10^{-7}
308	4.312×10^{-3}	4.312×10^{-4}	8.15×10^{-7}

Figure 4.7: I=7A

The average of rdr was taken and the results were plotted against B. The slope of the graph was found to be

$$k = (1.501 \pm 0.203) \times 10^{-6} \quad \Longleftrightarrow \quad \mu_B = \frac{khc}{\lambda n^2 f^2} = (9.4845 \pm 1.3032) \times 10^{-24} JT^{-1}.$$

The graph is shown below. To determine the polarisation state, we noted that at 0° the

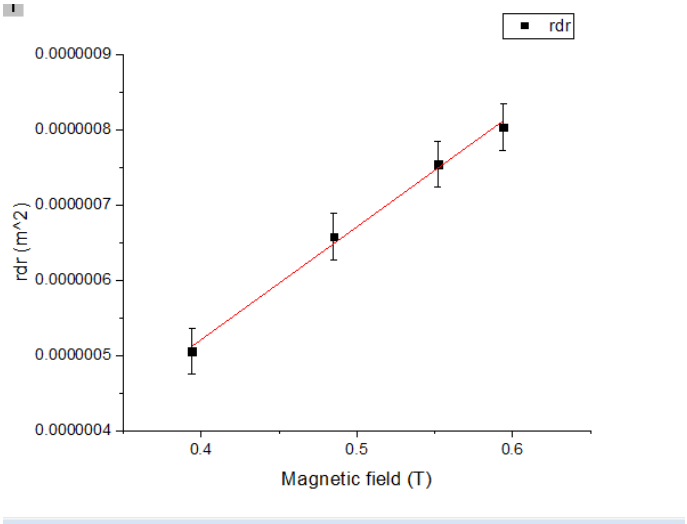

Figure 4.8: Graph of rdr against magnetic field strength

middle peak is muted, while at 90° the inner one is and the others remain. Thus the outer and inner peaks are perpendicularly polarised wrt each other.

4.3 Longitudinal Zeeman Effect

In this section we observed the splitting into double peaks. Following the methodology supplied earlier, I produced data in the same manner as before for I=5,7A. I found the value of $r\Delta r = (6.942 \pm 0.303) \times 10^{-7} m^2$, and $(8.605 \pm 0.405) \times 10^{-7} m^2$ respectively. These yielded values of $\Delta\lambda =$,
Using the values obtained for $r\Delta r$, we found values for $\Delta\lambda$ tabled below for both orientations for I=5,7A.

Calculation of $\Delta\lambda$ for Transverse and longitudinal configurations at 5A and 7A			
Current	Transverse	Longitudinal	Literature
5A	$(9.144 \pm 0.282)pm$	$9.420 \pm 0.451)pm$	$9.38pm$
7A	$(11.20 \pm 0.350)pm$	$11.39 \pm 0.541)pm$	$11.50pm$

To determine the polarisation state, we used the linear polariser and the quarter wave plate. We noticed that as we turned the the wave plate from 0-45° one of the peaks grew taller, and the other minimised. It was the opposite case when we went from 0-(-45)°. Plots of the intensity at both maxima and their equilibrium are below. This leads me to believe that each peak is left hand or right hand polarised, as they are 90° out of phase.

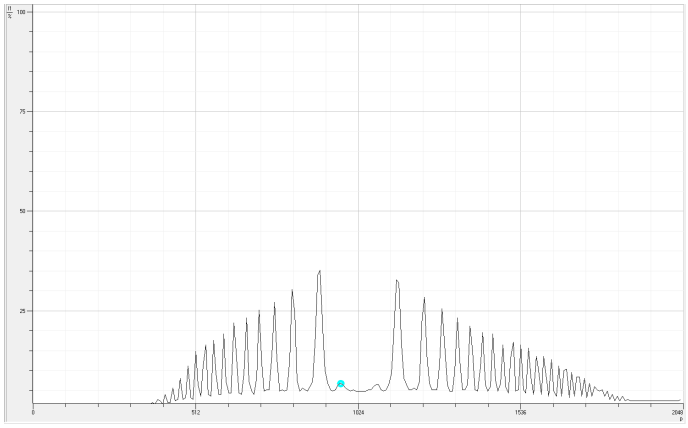

Figure 4.9: -45°

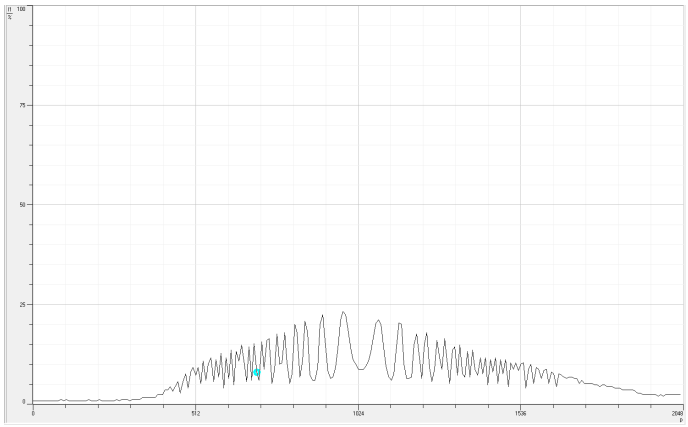

Figure 4.10: 0°

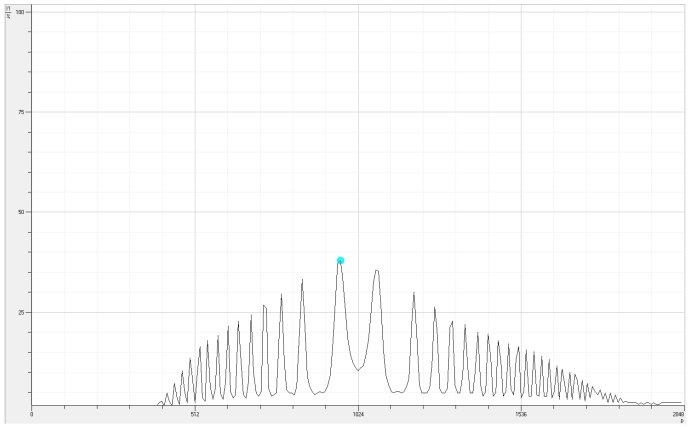

Figure 4.11: 45°

5 Error handling

- When measuring the specific height of the peak, there was an error in locating the precise point of maximum local intensity. Due to this we attributed a pixel error of ± 5
- We used the standard Gaussian error formulae for error propagation throughout.
- I found there to be systematic error in the experiment. This can be seen as our peaks were not symmetric, yet we were unable to right it.

6 Conclusion

We completed the goals of this experiment, although slight systematic errors were worked through. The Red line in Cadmium was found within experimental error. The triplet split was observed for the transverse Zeeman effect, and $\lambda \propto B$ from our graph 4.4. Also

the Bohr magneton was found from 4.4 to be within reasonable error. It was also found that the outer peaks were linerally polarisied perpendicular to the innermost peak.

For the longitudinal ZE, we observed doublet lines and were able to find values for $r\Delta r$ and they were within error of the corresponding transverse ZE values.Values for the shift in wavelenght $\Delta\lambda$, and they were found to corrospond to one another at a given current. We found after application of the linear, and quarter wave polariser that the doublet lines were circularly polarised at 90° to each other.

References

[1] Wavelenght Redline, last opened 9/2/2020:
https : *//www.rp − photonics.com/standard*$_s$*pectral*$_l$*ines.html*

[2] Bohr Magnetonhttps, last opened 9/2/2020:
//physics.nist.gov/cgi − bin/cuu/Value?mub

[3] Paschen-Bach effect, last opened 9/2/2020:
http : *//hyperphysics.phy − astr.gsu.edu/hbase/quantum/paschen.html*

7 Appendix

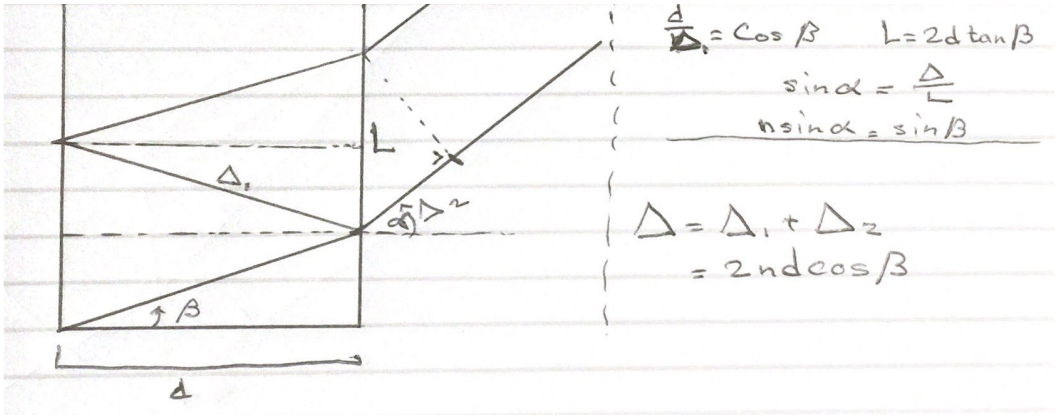

Figure 7.1: Proof 1

7.1 Intensity graphs

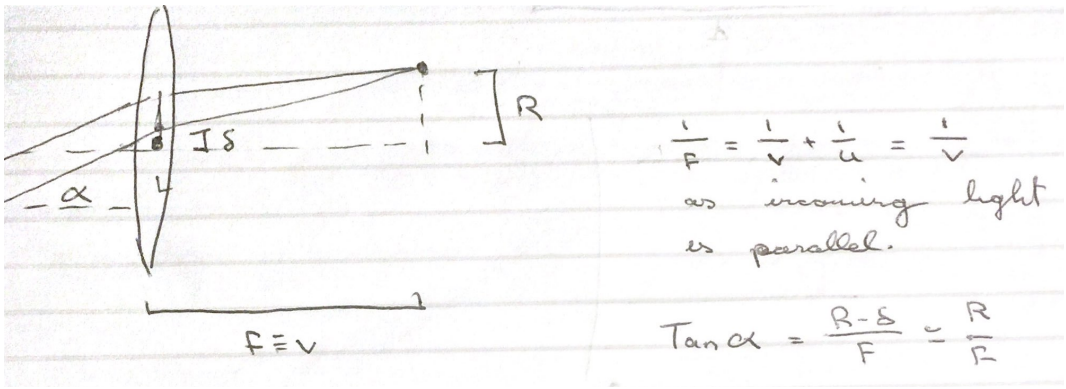

Figure 7.2: Proof 2

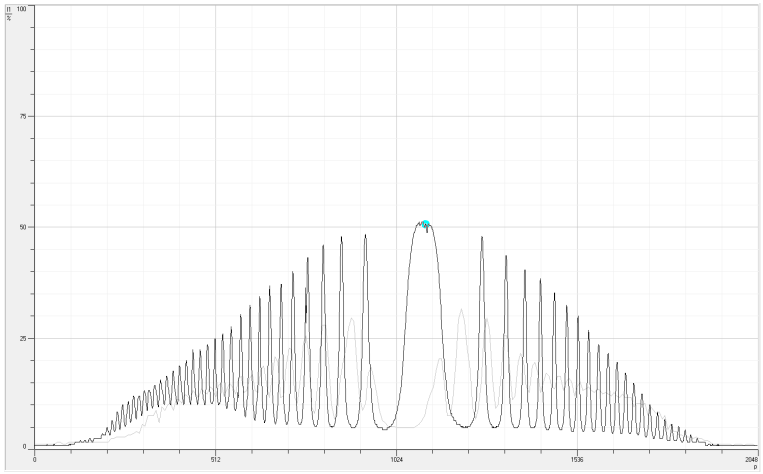

Figure 7.3: B=0 peaks

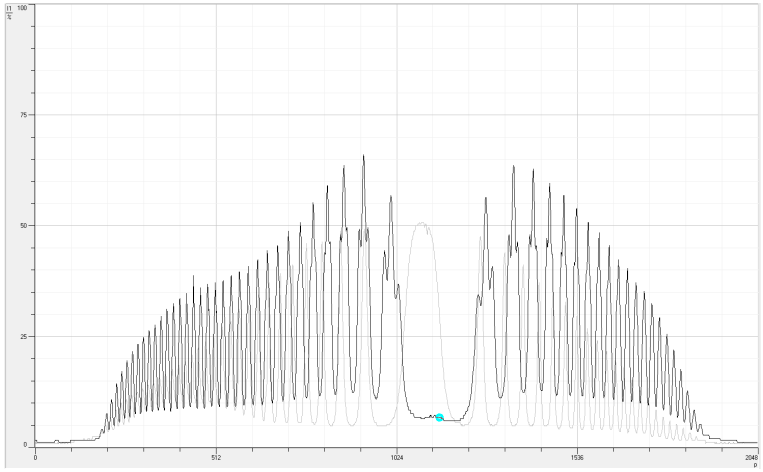

Figure 7.4: I=4A peaks

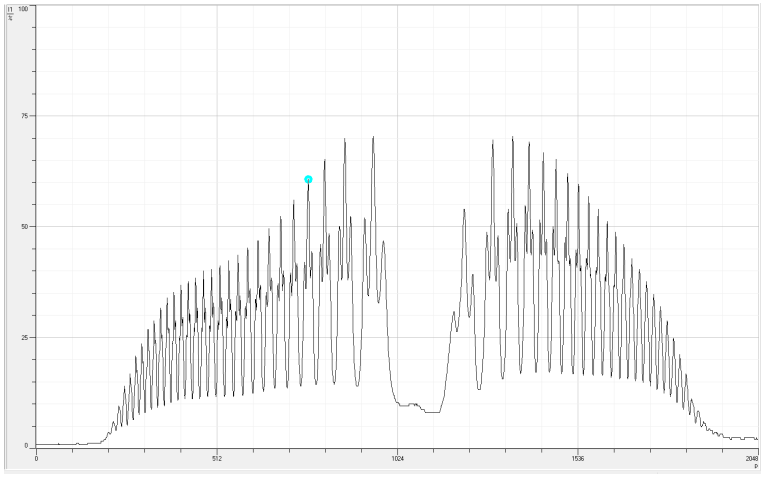

Figure 7.5: I=5A peaks

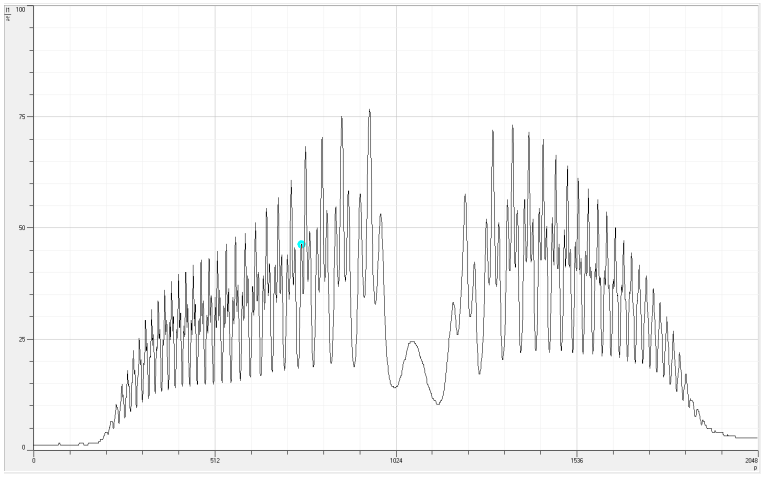

Figure 7.6: I=6A peaks

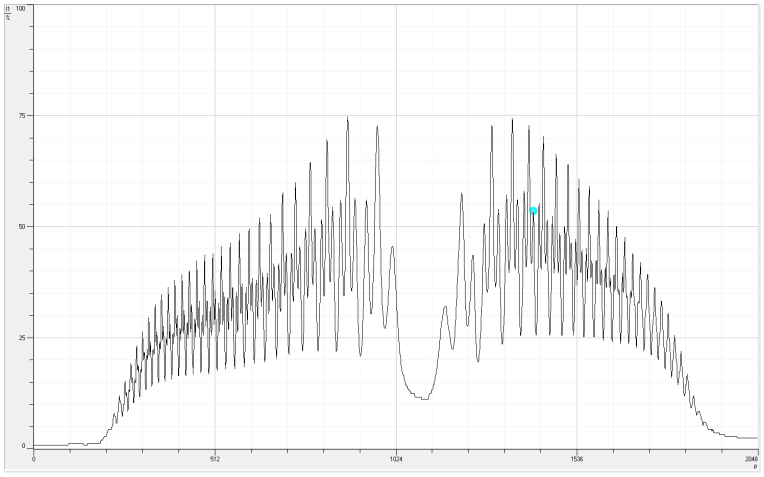

Figure 7.7: I=7A peaks